 https://doi.org/10.3311/PPci.23657

Periodica Polytechnica Civil Engineering, 69(2), pp. 382–396, 2025

Plate Buckling Assessment of Unstiffened and Uniaxial Compressed Plates through Overall Imperfection Method

Mohammad Kheer Alewe[1*]

[1] Department of Structural Engineering and Geotechnics, Faculty of Architecture, Civil Engineering and Transport Sciences, Széchenyi István University, Egyetem tér 1., H-9026 Győr, Hungary
[*] Corresponding author, e-mail: alewe.mohammad.kheer@sze.hu

Received: 17 October 2023, Accepted: 26 November 2024, Published online: 03 January 2025

Abstract

The Overall Imperfection Method (OIM) is a more comprehensive version of the Unique Global and Local Imperfection Method introduced for steel column design in EN 1993-1-1 standard. The generalized OIM is used to evaluate the stability resistance of steel members subjected to irregular load conditions. This study extensively examines the Overall Imperfection Method (OIM) used in analyzing plate buckling, explicitly focusing on steel grades such as S235, S355 and S460. It compares OIM with methods mentioned in EN 1993-1-5 (Annex B, GMNIA and winter curve). The research carefully validates OIM by analyzing Equation (13) (Annex B) across ratios and studying its behavior with various steel grades. The study highlights the importance of finding a balance when applying OIM regarding material properties and slenderness ratios. These findings provide insights for engineering professionals. Additionally, the research introduces a calibrated equation that allows for the application of OIM without exceeding the limits set by GMNIA. This simplifies its implementation in engineering practice.

Keywords

equivalent initial imperfection, overall imperfection method, plate buckling, flexural buckling, reduced stress method, GMNIA, GNIA, modified equivalent amplitude

1 Introduction

1.1 General

Buckling is the main problem that many steel structural members suffer from, leading to decreased strength and loss of stability. There are two main types of buckling: global buckling and local buckling. For global buckling two alternative standardized methods are available to evaluate the resistance of steel members subjected to either uniform or no uniform loading. These are the General Method (EN 1993-1-1 [1]: paragraph 6.3.4; referred as GM) and the Overall Imperfection Method (EN 1993-1-1 [1]: paragraph 5.3.2(11); referred as OIM). However, both methods have common theoretical bases.

The OIM is the generalization of the Unique Global and Local Imperfection (referred as UGLI) method, which is introduced by the EN 1993-1-1 standard [1] and published by Chladný and Štujberová [2]. The original UGLI is valid for structural members subject to flexural buckling. Later, Agüero et al. [3] generalized the UGLI method for lateral-torsional buckling, and Papp [4] extended the method to structural members sensitive to the interaction between flexural and lateral-torsional buckling. The application of the OIM was introduced in [5] for beam-columns with a greater variety of load conditions. In addition, the accuracy of the procedure was evaluated for beam columns subjected to various stress conditions [6]. It was discovered that the OIM for structural member is safe and has a comparable level of safety to existing design methodologies. Szalai and Papp [7] published the most comprehensive description of the generalized OIM. Papp et al. [8] utilized the OIM to design irregular structural members and simple portal frames. Eventually, Nemer et al. [9] expanded the use of OIM for structural members at elevated temperatures.

All previous research has focused entirely on using the OIM for the design of steel beam-column members in the case of global buckling. However, the EN 1993-1-5 [10] provides simplified methods for designing plated steel structures in the case of plate buckling, such as the Effective Width Method (referred to as EWM) and the Reduced Stress Method (referred as RSM). The aim of this

Cite this article as: Alewe, M. K. "Plate Buckling Assessment of Unstiffened and Uniaxial Compressed Plates through Overall Imperfection Method", Periodica Polytechnica Civil Engineering, 69(2), pp. 382–396, 2025. https://doi.org/10.3311/PPci.23657

study is to examine whether the RSM and the OIM can be extended to the assessment of plate buckling and what about the accuracy of the methods.

1.2 OIM for buckling of beam-columns

As mentioned above, the current antecedent of the OIM defined in clause 5.3.2(11) of EN 1993-1-1 [1] is limited to members with flexural buckling mode due to pure compression only. This regulation defines the amplitude of the overall geometrical imperfections having the shape of the relevant buckling mode resulting from the linear buckling analysis (LBA), and the equivalent amplitude of the initial geometrical imperfection is defined as follows:

$$\upsilon_{init,\max} = \frac{e_{0d}}{\bar{\lambda}^2}\frac{N_{Rk}\upsilon_{cr,\max}}{EI\upsilon''_{cr,\max}} \tag{1}$$

where the equivalent initial amplitude belongs to the Ayrton-Perry formulation calibrated by Maquoi and Rondal [11]:

$$e_{0d} = \alpha\left(\bar{\lambda} - 0.2\right)\frac{W}{A} \quad \text{for } \bar{\lambda} > 0.2 \tag{2}$$

and where:

- $\upsilon_{cr,\max}$ is the magnitude corresponding to the shape of the elastic flexural buckling mode.
- $EI\upsilon''_{cr,\max}$ is the moment of internal bending produced by the υ_{cr} buckle deformation.
- The $\bar{\lambda}$ is the decreased slenderness for flexural buckling mode.
- N_{Rk} is the capacity to withstand the distinctive axial force with consideration to the categorization of the cross-sectional shape.
- The α is the factor accounting for imperfections in the context of the flexural buckling curve.
- The e_{0d} is the comparable magnitude of initial imperfections manifested in the shape of a buckling mode, specifically for the fundamental scenario of flexural buckling.
- W and A are the elastic cross-sectional properties.

The idea and the application of the method have been published by Chladný and Štujberová in [2]. Fig. 1 shows the reference member for the flexural buckling mode, where $\upsilon_{init}(x)$ is the shape of the imperfect member and $\upsilon(x)$ is the deformation caused by the N_{Ed} compressive force. The $\upsilon_{init}(x)$ can be written as follows:

$$\upsilon_{init}\left(x\right) = \upsilon_{init,\max}\frac{\upsilon_{cr}\left(x\right)}{\upsilon_{cr,\max}}. \tag{3}$$

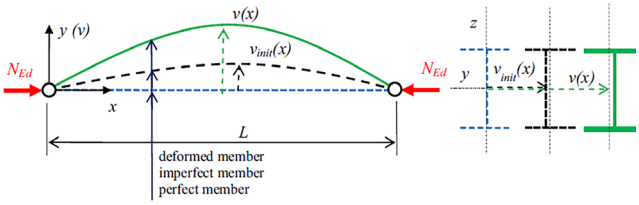

Fig. 1 Fundamental case (reference member) for flexural buckling mode [4]

In Eq. (3) $\upsilon_{cr}(x)$ is the shape of the elastic buckling mode and $\upsilon_{cr,\max}$ is the amplitude with arbitrary value. The $\upsilon_{init,\max}$ is the amplitude of the equivalent initial imperfection. The second-order deformation can be expressed by linear approach:

$$\upsilon^{II}\left(x\right) = \upsilon_{init}\left(x\right)\frac{1}{\alpha_{cr} - 1} \tag{4}$$

where α_{cr} is the critical load factor. The second order bending moment is as follows:

$$M^{II}_{\upsilon_{init}}\left(x\right) = EI\left(\upsilon^{II}\left(x\right)\right)'' = \upsilon_{init,\max}\frac{1}{\alpha_{cr} - 1}\frac{EI}{\upsilon_{cr,\max}}\upsilon''_{cr}\left(x\right). \tag{5}$$

Considering the following equations,

$$\sigma^{II}_{\upsilon_{cr},\max} = \frac{M^{II}_{\upsilon_{cr},\max}}{W}$$

$$\upsilon^{II}_{\max} = \frac{1}{\alpha_{cr} - 1}\upsilon_{cr,\max}$$

$$\sigma^{II}_{\upsilon_{init},\max} = \frac{M^{II}_{\upsilon_{init},\max}}{W} = \frac{e_{0d}\dfrac{\alpha_{cr}}{\alpha_{cr} - 1}N_{Ed}}{W} \tag{6}$$

the initial imperfection of Eq. (3) can be obtained as follows [4]:

$$\upsilon_{init}\left(x\right) = \frac{\sigma^{II}_{\upsilon_{init},\max}}{\sigma^{II}_{\upsilon_{cr},\max}}\upsilon_{cr}\left(x\right). \tag{7}$$

Where the symbols are defined as follows:

- $\sigma^{II}_{\upsilon_{cr,\max}}$ is the maximum second-order normal stress from bending as the effect of the N_{Ed} compressive force with initial imperfection in the shape of the elastic buckling mode with arbitrary amplitude $\upsilon_{cr,\max}$;
- $\sigma^{II}_{\upsilon_{init,\max}}$ is the maximum second-order normal stress from bending as the effect of the N_{Ed} compressive force with the calibrated value of the equivalent amplitude, considering Eq. (2).

Papp in [4] derived the equivalent amplitude υ_{0d} for the reference case of LTB and showed that the formula of Eq. (7) is valid for lateral-torsional buckling mode too. Moreover, Papp [4] showed that the equivalent amplitude $\upsilon_{0d,NM}$ derived

for case of coupled buckling mode (Szalai et al., cited in Papp [4:pp.125, 128, 135]) provides reasonable accuracy:

$$\upsilon_{0d,NM} = \frac{\alpha_{ult}}{\alpha_{ult,N}} e_{0d} + \frac{\alpha_{ult}}{\alpha_{ult,M}} \upsilon_{0d},$$

where

$$\alpha_{ult,N} = \frac{N_{Rk}}{N_{Ed}};\ \alpha_{ult,M} = \frac{M_{y,Rk}}{M_{y,Ed}};\ \alpha_{ult} = \frac{1}{\frac{1}{\alpha_{ult,N}} + \frac{1}{\alpha_{ult,M}}}. \quad (8)$$

Furthermore, for irregular member conditions Papp [4:p.129] used the following working hypothesis:

"In case of a member with irregular conditions (arbitrary supports; non-uniform cross-section; non-uniform distribution of internal forces), the $\sigma^{II}_{\upsilon_{init,\max}}$ maximum second-order normal stress due to bending around the z axis and warping may be calculated on the reference member. The reference member has the calibrated equivalent amplitude as well as load, cross-section and critical load taken into account in the reference point of the member. The reference point coincides with the cross-section where the $\sigma^{II}_{\upsilon_{cr,\max}}$ second-order normal stress due to bending and warping as effects of the load with equivalent initial imperfection in the shape of the buckling mode with arbitrary amplitude has maximum value."

The control calculations and later wide range numerical verifications justified his assumption.

1.3 Aim of the research

The study's main goal was to evaluate the Overall Imperfection Method (OIM) in analyzing plate buckling and its effectiveness with different types of steel. The researchers compared it to established methods outlined in EN 1993-15 [10], such as GMNIA, winter curve and Annex B of [10]. By examining OIMs' behavior related to slenderness; they identified situations where it either erred on the side of caution or fell short. Additionally, they extensively studied how material changes affected OIM predictions. One noteworthy achievement of this study was the creation of a linear equation that makes it easier to apply OIM in practice while ensuring accuracy within GMNIA limits.

2 Plate buckling design by EC3

2.1 General

In shipbuilding, thin-walled constructions, and construction industries, the phenomena of plate buckling caused by in-plane compressive or/and shear stress are important. Plate buckling may lead to a sudden and catastrophic failure, such as the collapse of the entire structure or a portion of it. Buckling is a significant issue, especially in thin-walled structures where the membrane rigidity is significantly greater than the bending stiffness [12]. The buckling resistance of steel-plated structures is specified in the EN 1993-1-5 standard [10]. The standard proposes the following specific methods to calculate the plate buckling resistance:

- Effective Width Method (EWM);
- Reduced Stress Method (RSM) or Overall Imperfection Method (OIM);
- Geometrically and Materially Nonlinear Analysis with Imperfections (GMNIA).

The EWM approach is relevant for traditional manual calculation, and it is out of the focus of this paper, while GMNIA is mostly a tool for researchers. However, engineering practice requires an intermediate approach using Geometric Nonlinear elastic Analysis with imperfection (GNIA), Linear Buckling Analysis (LBA) and buckling curve developed for reference plate buckling. RSM or alternatively the OIM are these types of design approach.

2.2 Design methods

2.2.1 General method

The Reduced Stress Method (RSM) may be used to determine stress limits for stiffened or unstiffened plates. The formula is specified in Section 10 of EN 1993-1-5 [10]. The RSM design formula is similar to the General Method introduced by the Section 6.3.4 of EN 1993-1-1 [1] for beam-columns:

$$\frac{\rho \alpha_{ult,k}}{\gamma_{M1}} \geq 1 \quad (9)$$

In Eq. (9) $\alpha_{ult,k}$ is the minimum load amplifier for the design load to reach the characteristic value of the yielding resistance in the critical point of the plate without plate buckling taking into account,

$$\alpha_{ult,k} = \frac{f_y}{\sigma_{eq,Ed}} \quad (10)$$

where the equivalent stress can be calculated as follows [13]:

$$\sigma_{eq,Ed} = \sqrt{\sigma^2_{x,Ed} + \sigma^2_{z,Ed} - \sigma_{x,Ed}\sigma_{z,Ed} + 3\tau^2_{Ed}}. \quad (11)$$

In Eq. (9) ρ is the reduction factor which may be calculated according to the Annex B of EN 1993-1-5 [10] informative formula:

$$\rho = \frac{1}{\varphi_p + \sqrt{\varphi_p^2 - \bar{\lambda}_p}} . \tag{12}$$

Where $\varphi_p = \frac{1}{2}\left(1 + \alpha_p\left(\bar{\lambda}_p - \bar{\lambda}_{p0}\right) + \bar{\lambda}_p\right)$ and $\bar{\lambda}_p = \sqrt{\frac{\alpha_{ult,k}}{\alpha_{cr}}}$

is the generalized plate slenderness. The values of $\bar{\lambda}_{p0}$ and α_p parameters can be found in Table 1. Computation of both $\alpha_{ult,k}$ and α_{cr} load amplifiers may be carried out by numerically using elastic shell finite element method.

2.2.2 Overall imperfection method

Additionally, to the general design method, the EN 1993-1-5 [10] alternatively proposes the overall imperfection method where the following equivalent amplitude can be used for the initial geometrical imperfection in the shape of the plate buckling mode (if $\gamma_{M1} = 1.0$):

$$e_0 = \alpha_p\left(\bar{\lambda}_p - \bar{\lambda}_{p0}\right)\frac{t}{6} \tag{13}$$

where t is the plate thickness. Using this equivalent geometrical imperfection, if the maximum normal stress computed by geometrically nonlinear elastic analysis (GNI) is equal to the characteristic yield stress, the plate buckling limit state is just reached: the evaluation of the plate buckling limit state can be drawn back to the evaluation of the first yielding limit state based on second order stress analysis. The second order stress analysis may be carried out by numerically using shell finite element analysis.

2.2.3 Geometrically and materially nonlinear analysis with imperfection

In case of plate panels, for the geometrically and materially non-linear analysis (GMNIA) characteristic values for the model parameters are mostly used, consequently the shell or even more complex finite element methods are capable to directly capture the design value of the local buckling phenomenon. This requires the consideration of material nonlinearities. According to the Annex C of EN 1993-1-5 [10] the geometrical imperfection can be considered with $b/200$ amplitude, where b is the width of the unstiffened panel. For the shape of the geometrical imperfection the relevant buckling modes can be used. Besides this geometrical imperfection, if the panel is part of a cross-section (e.g., it is the web plate of an I cross-section) residual stress should also be applied for the numerical model.

Table 1 Values for $\bar{\lambda}_{p0}$ and α_p parameters

Product	Predominate buckling mode	α_p	$\bar{\lambda}_{p0}$
Hot rolled	Direct stress for $\psi \geq 0$	0.13	0.7
	Direct stress for $\psi < 0$		0.8
	Shear stress		0.8
	Transverse stress		0.8
Welded or cold-formed	Direct stress for $\psi \geq 0$	0.34	0.7
	Direct stress for $\psi < 0$		0.8
	Shear stress		0.8
	Transverse stress		0.8

2.3 Working example

Simply supported square plate subjected to uniaxial compressive stress (ψ = 1) shown in Fig. 2 will be analyzed using the EC3 conform methods presented in Section 2.2. The dimensions of the plate are $a = b = 1500$ mm ($\alpha = a/b = 1$) and the plate thickness is t = 8 mm. The parameters of the applied bi-linear material are as follows: $E = 210000$ N/mm^2, $G = 80700$ N/mm^2, $f_y = 355$ N/mm^2 and $E/10000$ hardening slope. The design line load is p = 719.22 N/mm.

2.3.1 Applied numerical model

Fig. 3 [14] illustrates the meshing and support system employed for the panel under examination. This model served as the basis for conducting various analyses in this paper, where it was applied changing of the value of the slenderness (b/t) from 375 to 30. Fig. 4 illustrates the accuracy of the model. The vertical axis of Fig. 4 represents the buckling reduction factor (ρ), while the horizontal axis denotes the relative slenderness ($\bar{\lambda}_p$). In the study of Zizza [15] the slenderness b/t was varied from 30 to 250 by altering the plate's dimensions while maintaining a constant thickness of 6 mm. For example, when b/t = 250,

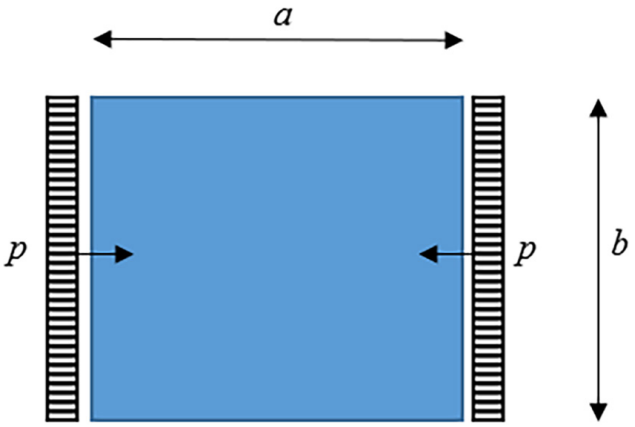

Fig. 2 The examined simple supported square plate panel

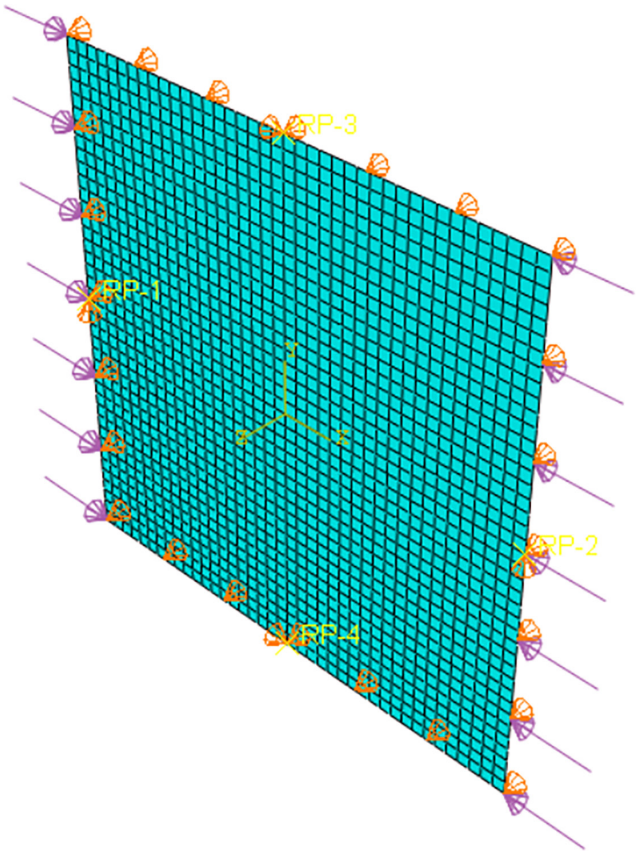

Fig. 3 Finite element model of the examined simply supported square plate (Abaqus [14] shell FE model with S4R shell element)

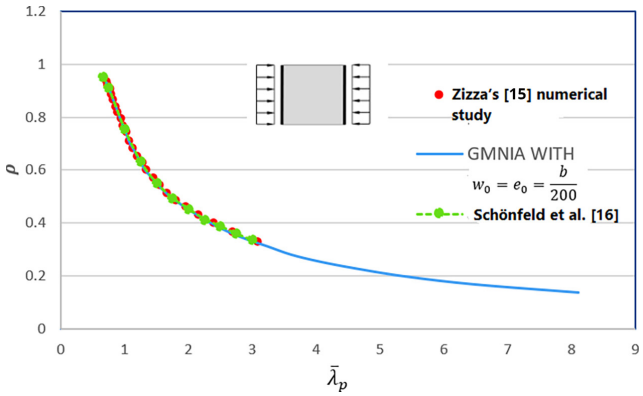

Fig. 4 Validation of the applied numerical model by Zizza's [15] results and Schönfeld et al. [16]

the plate's dimensions were set as $a = b = 1500$ mm with thickness of 6 mm. Also, Schönfeld et al. [16] used the same material and boundary conditions and stress ration of Zizza's [15] study, he was applied different shape of imperfections but in current study it will concentrate on uses just equivalent geometric imperfection when applying GMNIA. The used boundary condition prevents the nodes to move along the loaded edge freely, this type of boundary conditions have been used before by Braun [17] and Rusch and Lindner [18] because of they gave the best corresponding with winter curve. The amplitude of the geometrical imperfection in the shape of the plate buckling mode was $b/200$ same as assumed by Zizza [15], (see the Annex C in EN 1993-1-5 [10]). One can see that GMNI analysis gave the same buckling curve as Zizza's [15] computations. Therefore, the author bases the computations presented in this paper on this numerical model.

Using the validated model, the buckling resistance of the examined panel will be calculated using the different EC3 methods (see Section 2.2).

2.3.2 Buckling resistance by RSM

The reduced stress method (RSM) introduced by EN 1993-1-5 [10] has the following steps:

1. Step 1: Minimum load amplifier
   The equivalent stress and the minimum load amplifier can be computed with first order stress analysis (Eq. (10) and Eq. (11)):

$$\sigma_{eq,Ed} = 89.9 \ \text{N/mm}^2$$

$$\alpha_{ult,k} = \frac{f_y}{\sigma_{eq,Ed}} = \frac{355 \ \text{N/mm}^2}{89.9 \ \text{N/mm}^2} = 3.95 \, .$$

2. Step 2: Critical load amplifier
   Executing linear buckling analysis (LBA) the critical load amplifier and the buckling shape are obtained (Fig. 5):

$$\alpha_{cr} = 0.24 \, .$$

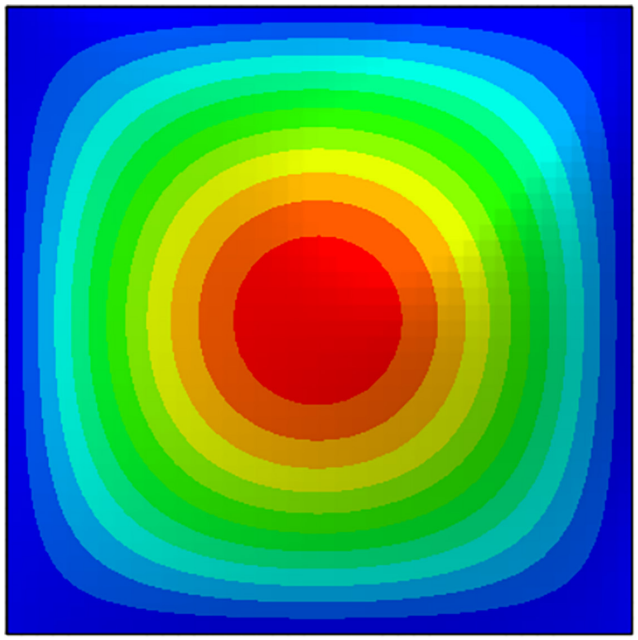

Fig. 5 Critical load amplifier and buckling mode

3. Step 3: Reduced plate slenderness
   According to the results of Step 1 and Step 2, the reduced plate slenderness is as follows:

$$\bar{\lambda}_p = \sqrt{\frac{\alpha_{ult,k}}{\alpha_{cr}}} = \sqrt{\frac{3.95}{0.24}} = 4.0567 .$$

4. Step 4: Buckling reduction factor
   The buckling reduction factor can be calculated with Eq. (12) using the slenderness given in Step 3 and the following parameters obtained from Table 1:

$$\alpha_p = 0.34 \text{ and } \bar{\lambda}_{p0} = 0.7$$

$$\varphi_p = \frac{1}{2}\left(1 + \alpha_p\left(\bar{\lambda}_p - \bar{\lambda}_{p0}\right) + \bar{\lambda}_p\right) = 3.099$$

$$\rho = \frac{1}{\varphi_p + \sqrt{\varphi_p^2 - \bar{\lambda}_p}} = 0.1833 .$$

5. Step 5: Buckling resistance
   The starting design load causes the following utilization of the buckling resistance (Eq. (9)):

$$U_{\text{RSM}} = \frac{\gamma_{M1}}{\rho\alpha_{ult,k}} = \frac{1.0}{0.1833 \times 3.95} = 1.381 > 1 \text{ not ok} .$$

   If the above utilization U is just 1.0, the applied is the buckling resistance $q_{b,\text{RSM}}$. This leads to an iterative procedure:

$$q_{b,\text{RSM}} = 520.7 \text{ N/mm}^2 .$$

2.3.3 Buckling resistance by OIM

The overall imperfection method (OIM) introduced by EN 1993-1-5 [10] has the following steps:

1. Step 1: Minimum load amplifier
   The equivalent stress and the minimum load amplifier can be computed with first order stress analysis (Eq. (10) and Eq. (11)):

$$\sigma_{eq,Ed} = 89.9 \text{ N/mm}^2 .$$

2. Step 2: Critical load amplifier

$$\alpha_{cr} = 0.24$$

3. Step 3: Reduced plate slenderness
   According to the results of Step 1 and Step 2, the reduced plate slenderness is as follows:

$$\bar{\lambda}_p = \sqrt{\frac{\alpha_{ult,k}}{\alpha_{cr}}} = \sqrt{\frac{3.95}{0.24}} = 4.0567 .$$

4. Step 4: Equivalent amplitude (e_0)
   According to Step 3 and the Eq. (13) it can calculate the equivalent amplitude as follows:

$$e_0 = \alpha_p\left(\bar{\lambda}_p - \bar{\lambda}_{p0}\right)\frac{t}{6} = 0.34\left(4.0567 - 0.7\right)\frac{8}{6}$$
$$= 1.5217 \text{ mm}.$$

5. Step 5: Calculate the maximum stress by applying GNIA with e_0 as imperfection
   In this stage, GNIA will assess the maximum stress and then compare it to the yield stress. To obtain reliable results, the maximum stress needs to be either less than or equal to the yield stress. Regrettably, it was observed that the maximum stress exceeded the yield stress, as illustrated in Fig. 6. This implies that the applied load, calculated using GMNIA, surpasses the ultimate load determined by OIM.

$$\sigma_{\max,\text{OIM}} = 520.2 > 355 \text{ NOT OK}$$

6. Step 6: Determine the ultimate load of OIM
   It was applied iteration by Python program [19] to reach to the ultimate load of OIM ($q_{ult,\text{OIM}}$ = 584.5) where the maximum stress equal to yielding stress ($\sigma_{\max,\text{OIM}} = f_y$ = 355 MPa) as shown in Fig. 7.

2.3.4 Buckling resistance by GMNIA

It was utilizing GMNIA to calibrate the RSM and OIM results. According to Annex C of EN 1993-1-5 [10] and [13]. To apply GMNIA, it was applied equivalent geometric imperfection as mentioned in Section 2.3.1 in the shape of buckling mode (Table 2).

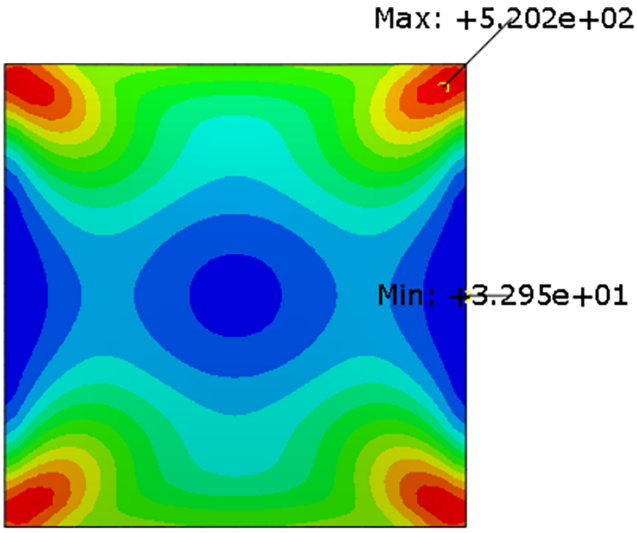

Fig. 6 Position and value of the maximum stress by applying GNIA with e_0 (in case of t = 8 mm)

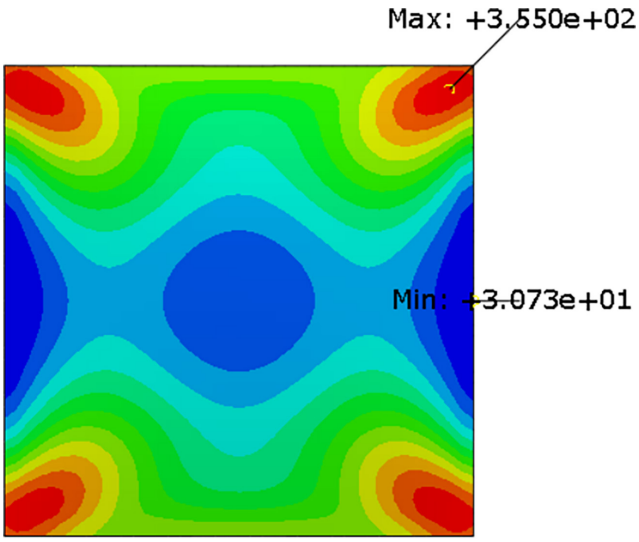

Fig. 7 Position and value of the maximum stress by applying GNIA with e_0 (in case of t = 8 mm)

Table 2 Values of geometric imperfections that are used in GMNIA

t (mm)	b/t	e_0 (mm) = b/200 Annex C [10]
8	187.5	7.5

Fig. 8 depicts the correlation between the maximum load achieved by GMNIA and the corresponding maximum displacement. It is evident that the maximum load, denoted as $q_{ult,GMNIA}$, equals 719.22 N/mm. Additionally, the ultimate load value in Annex B of [10] is the most conservative, being the lowest among all. Furthermore, the ultimate load in OIM is noticeably distant from GMNIA and WINTER, but it is somewhat closer to Annex B of [10], with a difference of approximately 12.4%. In summary, GMNIA yields results more significant than any other method when dealing with slender plates. At the same time, Annex B of EN 1993-1-5 [10] produces the lowest values—conversely, employing the e_0 Eq. (13) mentioned earlier results in a more conservative outcome than GMNIA or Winter. This suggests that further verification is necessary to determine the suitable range of applications for the equation derived by Müller [20].

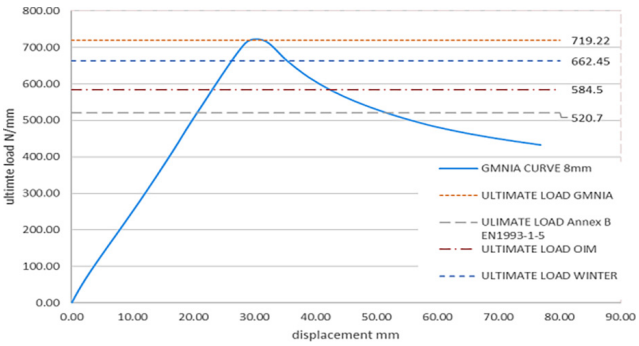

Fig. 8 Load vs. displacement curve obtained of GMNIA (in case of t = 8 mm)

Fig. 9 shows the distribution of stresses at the ultimate buckling load of GMNIA.

2.4 Literature review about equivalent geometric imperfection in plate buckling

Equivalent geometric imperfections in unstiffened plate buckling have been extensively examined. In a study by Schönfeld et al. [16], the ultimate load resulting from compressive stress was compared using various methods to account for imperfections. It was observed that adjusted equivalent geometric imperfections achieved favorable agreement with the Winter curve in the construction industry [16]. Paudel et al. [21] conducted an investigation on the impact of random initial geometric imperfections on the buckling limit load of composite cylindrical shells. They emphasized the significance of considering geometric imperfections during the design phase [21]. Zhang et al. [22] proposed a novel analytical model to address the buckling problem of plates with uncertain initial geometric imperfections. They utilized a double trigonometric series to depict the imperfections [22]. In a study by Liu et al. [23], the nonlinear dynamic response of thermally loaded composite plates with initial geometric imperfections was analyzed. The findings revealed that the imperfections delayed the onset of the critical state [23]. Zingoni [24] employed the concept of equivalent geometric imperfections to assess the buckling resistance of beams subjected to bi-axial bending. They suggested modifications to the predictions of critical moments [24].

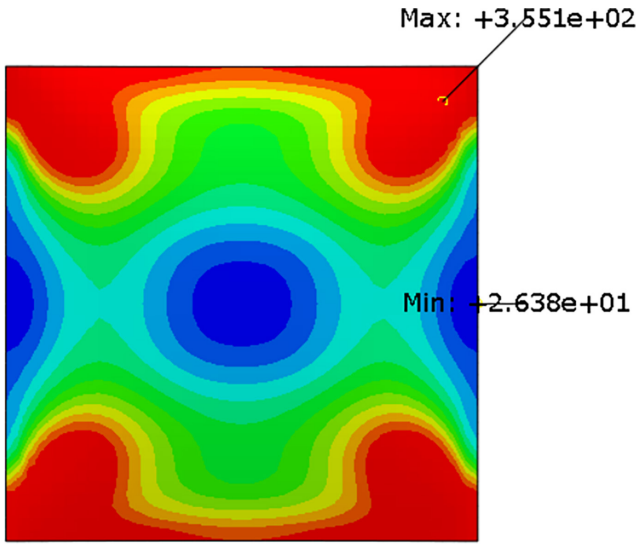

Fig. 9 Distribution stress at the ultimate buckling load of GMNIA

On the other hand, the Geometrical and Materially Nonlinear Imperfection Analysis (GMNIA) technique is utilized to identify equivalent geometric imperfections for local buckling of slender box-section columns. The aim of this technique is to estimate the interaction buckling resistance of high-strength steel box-section columns by incorporating equivalent imperfections in nonlinear plastic analysis. In order to find these equivalent imperfections, Radwan and Kövesdi [25–28] and Wang et al. [29] conducted research and developed numerical models to perform parametric studies. These models were validated to ensure accurate estimation of buckling capacities. Subsequently, these accurate buckling capacities were used to calibrate equivalent local and global imperfection combinations that can be applied in Finite Element Method (FEM)-based design. To ensure the safety level of the design, the proposed imperfection combinations were also subjected to reliability assessment. The outcomes of these studies can be utilized to determine the accurate buckling resistance and facilitate the FEM-based design approach for slender box-section columns made of high-strength steel. All the previous studies tried to find an approximate equivalent geometric imperfection to calculate buckling resistance by applying GMNIA. In conclusion, this study will focus on verifying the equation mentioned in Annex B of [10] and finding modifications if applying it to the range of relative slenderness by GNIA.

2.5 Verify the Annex B of EN 1993-1-5

In this section, the study rigorously validates the previously mentioned equivalent amplitude Eq. (13). This verification process involves applying the ultimate load derived from GMNIA across a range of slenderness ratios (b/t, varying from 375 to 30) achieved by adjusting plate thickness (ranging from 4 to 50 mm). The procedures outlined in Section 2.3.3 are meticulously followed, maintaining material properties and plate dimensions. The intricate relationship between the maximum stress of OIM and the stress obtained by applying GNIA with e_0 (Eq. (13)) concerning the slenderness of both unstiffened and square plates is depicted in Fig. 10. Remarkably, $\sigma_{max,OIM}$ surpasses the yielding stress for slenderness values ranging from 375 to 60, achieving equilibrium at $b/t = 60$. This signifies that the ultimate load obtained from GMNIA exceeds OIM's ultimate load. Conversely, reducing the slenderness below 60 diminishes OIM's maximum stress, resulting in OIM's ultimate load surpassing that of GMNIA.

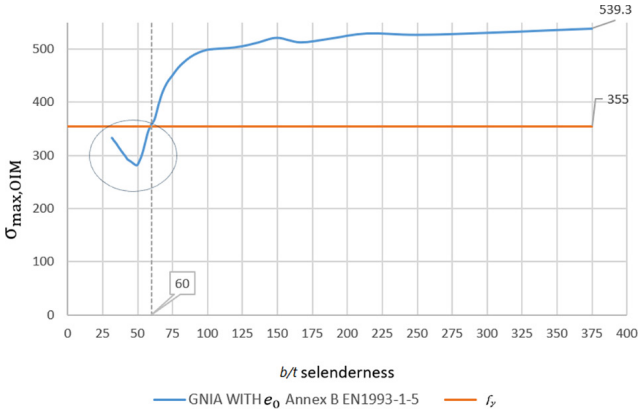

Fig. 10 Relation between the maximum stress of OIM and slenderness (b/t) in case of unstiffened and square plate

Based on identical values of e_0 (Eq. (13)), an investigation was conducted to determine the ultimate load, ensuring that the maximum stress remained below the yielding stress using Python [19] in conjunction with Abaqus [14]. Fig. 11 illustrates how the load varies with thickness for each method employed (Annex B of EN 1993-1-5 [10], Winter ($\psi = 1$), GMNIA with $e_0 = b/200$, and OIM (GNIA with e_0 (Eq. (13)))). Notably, the GMNIA method, incorporating equivalent geometric imperfections, aligns closely with the winter curve, as previously mentioned. Conversely, the ultimate load calculated by the guidelines outlined in Annex B of EN 1993-1-5 [10] yields the most conservative load values. Furthermore, ultimate load estimations based on the GNIA method, incorporating e_0 (Eq. (13)) as an imperfection, yield more conservative results than those obtained through the winter or GMNIA methods but more significant than the values from Annex B of [10]. Interestingly, at specific thickness values t = 25 mm, the load curve exhibits fluctuations

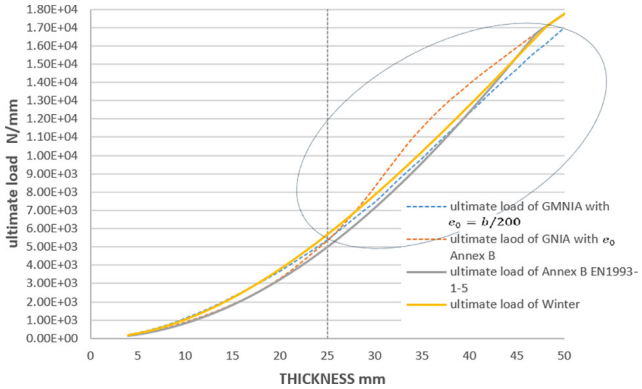

Fig. 11 Ultimate load of four methods (Annex B of EN 1993-1-5 [10], Winter ($\psi = 1$), GMNIA with $e_0 = b/200$, and OIM (GNIA with e_0 (Eq. (13))))

where the load exceeds that of the winter or methods. This suggests that the accuracy of e_0 in this scenario may need refinement to ensure that loading remains below the ultimate load of GMNIA.

To address the challenge, a systematic approach was adopted involving an iterative process to determine an accurate value of e_0, ensuring that the maximum stress aligns precisely with the yielding stress. By achieving this equilibrium, it was ascertained that the applied load remained well within the limits of the ultimate load derived from the GMNIA method. Fig. 12 visually depicts the correlation between the relative slenderness ($\bar{\lambda}_p$) and the adjusted imperfection parameter e_0. The primary objective of this correlation was to establish a direct link between imperfection and relative slenderness. The process involved transforming the actual structural behavior into a linear approximation across various ranges of relative slenderness (as illustrated in Fig. 12). This approach enables engineers dealing with compressive square plates to employ the GNIA method with the modified e_0, obviating the need for intricate analyses akin to GMNIA where this is the main goal of OIM. Consequently, this streamlined methodology translates to significant time and effort savings. The derived equations it will be as follows:

$$
\begin{aligned}
&\text{If } f_y = 355 \text{ MPa}, \ \alpha_p = 0.34, \ \bar{\lambda}_{p_0} = 0.7 \ \text{(Table 1)} \\
&1.08 \le \bar{\lambda}_p < 1.3 \\
&e_{0,\text{modified}} = 9.7 - 6.8\bar{\lambda}_p \\
&0.94 \le \bar{\lambda}_p < 1.08 \\
&e_{0,\text{modified}} = 4.466 - 1.95\bar{\lambda}_p \\
&0.8 \le \bar{\lambda}_p < 0.94 \\
&e_{0,\text{modified}} = 0.36 + 2.414\bar{\lambda}_p \\
&0.7 \le \bar{\lambda}_p < 0.8 \\
&e_{0,\text{modified}} = -3.077 + 6.71\bar{\lambda}_p .
\end{aligned}
\tag{14}
$$

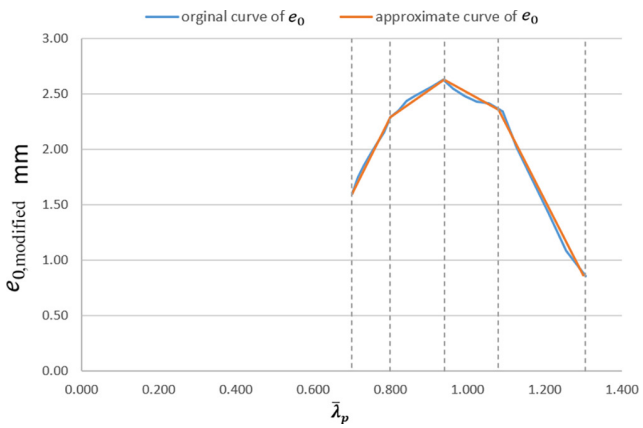

Fig. 12 Original and approximate curve of value of $e_{0,\text{modified}}$ in relationship with relative slenderness $\bar{\lambda}_p$

Utilizing the equations mentioned above, a noteworthy observation emerged: the reduction curve associated with the GNIA method, incorporating e_0, closely follows the reduction curve of GMNIA with $e_0 = b/200$. This alignment is particularly pronounced within the range of relative slenderness, reaching up to 1.3 and extending down to 0.7, as illustrated in Fig. 13.

2.5.1 Influence changes the material on the value of e_0 (Eq. (13))

In previous research, material properties played a pivotal role. Radwan and Kövesdi [25] explored this impact by formulating equivalent geometric imperfections for box section columns in various materials (S235, S355, S460). Additionally, Somodi et al. [30] conducted a numerical study comparing NSS (S235-S355) and HSS (S420-S960) to assess local buckling resistance in welded box sections. This study delves into three steel grades (S235, S355, S460) and analyzes their influence on the buckling curves of four methods, emphasizing the material's effect on the e_0 value.

2.5.2 Using steel grade S235

Fig. 14 illustrates the correlation between the reduction factor and relative slenderness for steel grade S355. The numerical study's buckling curve aligns well with the winter curve, while Annex B of EN 1993-1-5 [10] demonstrates a more conservative approach than winter or GMNIA. Fig. 15 depicts the relationship between the maximum stress of OIM and slenderness (b/t). Notably, the maximum stress of OIM equals the yielding stress at b/t = 75, mirroring the behavior observed in steel grade S355 (refer to Fig. 10). Fig. 16 reveals that the ultimate load of OIM surpasses (winter, GMNIA, or Annex B of [10]) values after a thickness of t = 20 mm (b/t = 75). Employing the methodology outlined in Section 2.5

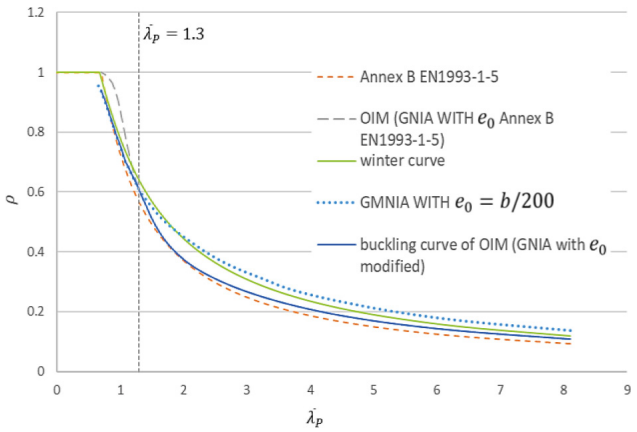

Fig. 13 Buckling curve of GMNIA, OIM with e_0, and OIM with $e_{0,\text{modified}}$ of unstiffened and square plate

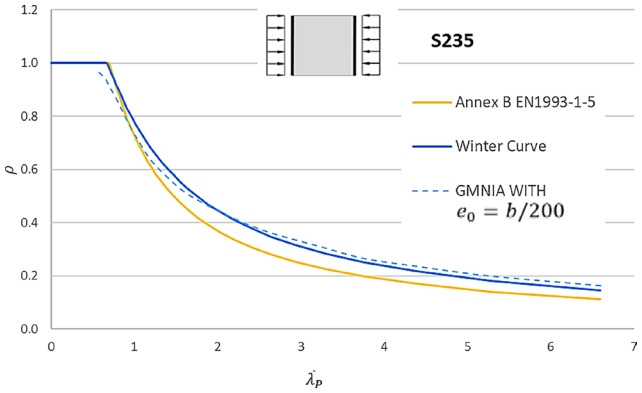

Fig. 14 Buckling curve of GMNIA, Winter, Annex B of unstiffened and square plate

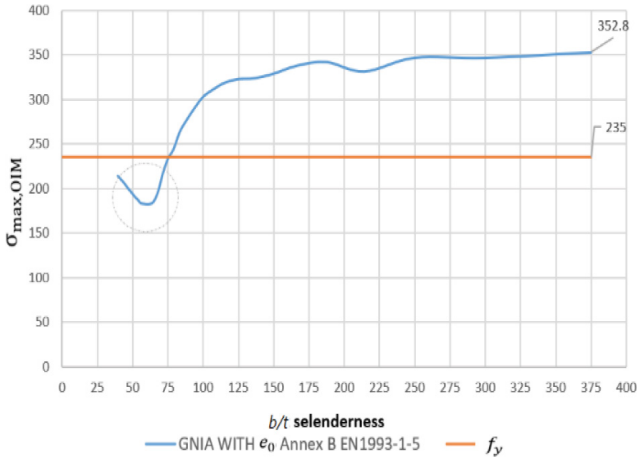

Fig. 15 Relation between the Maximum stress of OIM and slenderness (b/t) in case of unstiffened and square plate

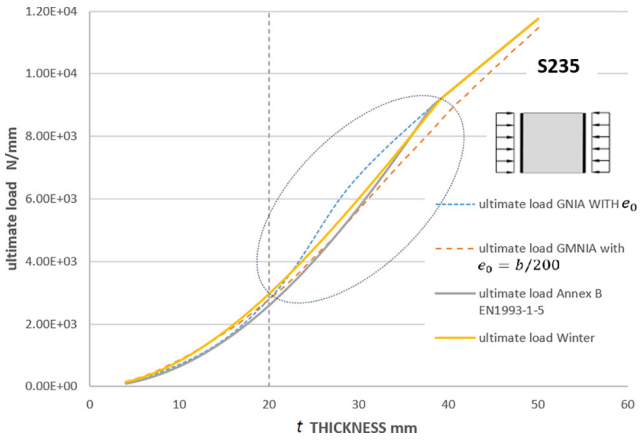

Fig. 16 Ultimate load of four methods (Annex B of EN 1993-1-5 [10], Winter ($\psi = 1$), GMNIA with $e_0 = b/200$, and OIM (GNIA with e_0 (Eq. (13))))

ensures an accurate determination of $e_{0,\text{modified}}$, preventing the maximum stress of OIM from exceeding the yielding stress as shown in Fig. 17. The derived equations it will be as follows:

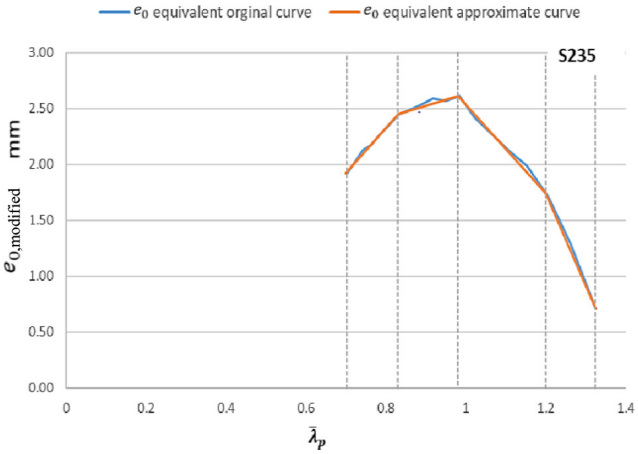

Fig. 17 Original and approximate curve of value of $e_{0,\text{modified}}$ in relationship with relative slenderness $\bar{\lambda}_p$

$$
\begin{aligned}
&\text{If } f_y = 355 \text{ MPa}, \ \alpha_p = 0.34, \ \bar{\lambda}_{p_0} = 0.7 \ \text{(Table 1)} \\
&1.2 \le \bar{\lambda}_p < 1.3 \\
&e_{0,\text{modified}} = 11.71 - 8.304\bar{\lambda}_p \\
&0.98 \le \bar{\lambda}_p < 1.2 \\
&e_{0,\text{modified}} = 6.465 - 3.93\bar{\lambda}_p \\
&0.83 \le \bar{\lambda}_p < 0.98 \\
&e_{0,\text{modified}} = 1.557 + 1.073\bar{\lambda}_p \\
&0.7 \le \bar{\lambda}_p < 0.83 \\
&e_{0,\text{modified}} = -0.917 + 4.054\bar{\lambda}_p .
\end{aligned}
\tag{15}
$$

Utilizing the equations mentioned above, a noteworthy observation emerged: the reduction curve associated with the GNIA method, incorporating e_0, closely follows the reduction curve of GMNIA with $e_0 = b/200$. This alignment is particularly pronounced within the range of relative slenderness, reaching up to 1.325 and extending down to 0.7, as illustrated in Fig. 18.

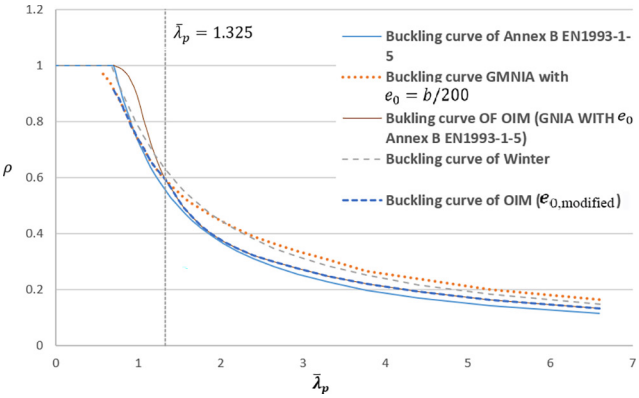

Fig. 18 Buckling curve of GMNIA, OIM with e_0, and OIM with $e_{0,\text{modified}}$ of unstiffened and square plate

2.5.3 Using steel grade S460

It can see the same observation that mentioned in the Section 2.5.2 (Fig. 14) as shown in Fig. 19. Fig. 20 depicts the relationship between the maximum stress of OIM and slenderness (b/t). Notably, the maximum stress of OIM equals the yielding stress at $b/t \approx 50$, mirroring the behavior observed in steel grade S355 (refer to Fig. 10). Fig. 21 reveals that the ultimate load of OIM surpasses (winter, GMNIA, or Annex B of [10]) values after a thickness of t = 29.5 mm ($b/t \approx 50$). Employing the methodology outlined in Section 2.5 ensures an accurate determination of $e_{0,\text{modified}}$, preventing the maximum stress of OIM from exceeding the yielding stress as shown in Fig. 22. The derived equations it will be as follows:

$$
\begin{aligned}
&\text{If } f_y = 460 \text{ MPa}, \ \alpha_p = 0.34, \ \bar{\lambda}_{p_0} = 0.7 \ \text{(Table 1)} \\
&1.2 \le \bar{\lambda}_p < 1.262 \\
&e_{0,\text{modified}} = 14.76 - 10.95\bar{\lambda}_p \\
&1 \le \bar{\lambda}_p < 1.2 \\
&e_{0,\text{modified}} = 7.24 - 4.685\bar{\lambda}_p \\
&0.9 \le \bar{\lambda}_p < 1 \\
&e_{0,\text{modified}} = 3.305 - 0.75\bar{\lambda}_p \\
&0.8 \le \bar{\lambda}_p < 0.9 \\
&e_{0,\text{modified}} = -0.934 + 3.96\bar{\lambda}_p \\
&0.7 \le \bar{\lambda}_p < 0.8 \\
&e_{0,\text{modified}} = -3.878 + 7.64\bar{\lambda}_p .
\end{aligned}
\tag{16}
$$

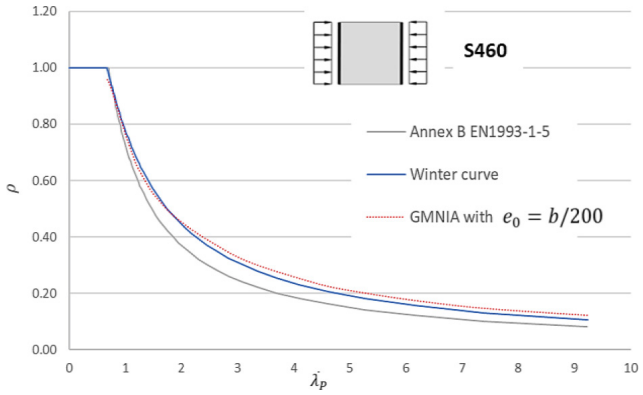

Fig. 19 Buckling curve of GMNIA, Winter, Annex B of unstiffened and square plate

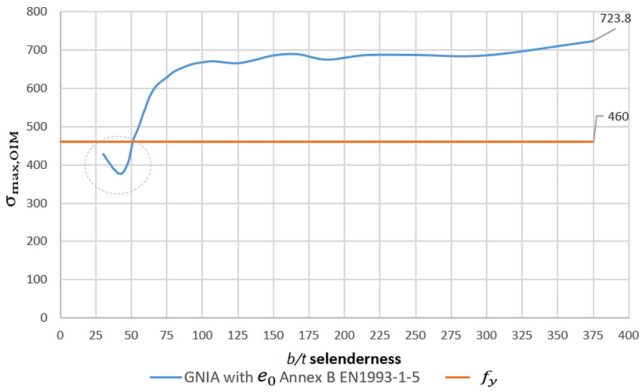

Fig. 20 Relation between the maximum stress of OIM and slenderness (b/t) in case of unstiffened and square plate

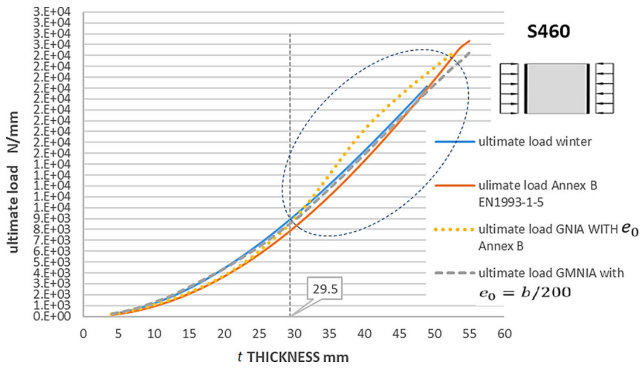

Fig. 21 Ultimate load of four methods (Annex B of EN 1993-1-5 [10], Winter (ψ = 1), GMNIA with $e_0 = b/200$, and OIM (GNIA with e_0 (Eq. (13))))

Utilizing the equations mentioned above, a noteworthy observation emerged: the reduction curve associated with the GNIA method, incorporating e_0, closely follows the reduction curve of GMNIA with $e_0 = b/200$. This alignment is particularly pronounced within the range of relative slenderness, reaching up to 1.262 and extending down to 0.7, as illustrated in Fig. 23.

3 Discussion the results

This study delved into applying the Overall Imperfection Method (OIM) in plate buckling, initially exploring its relevance in line beam-columns. The focus shifted to EN 1993-1-5 [10], comparing OIM with Annex B of [10], GMNIA, and the winter curve. The methodology was rigorously modelled and validated against prior research by Zizza [15] and Schönfeld et al. [16]. The paper extensively examined the

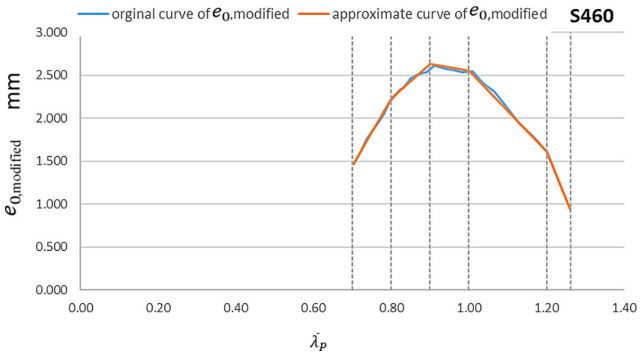

Fig. 22 Original and approximate curve of value of $e_{0,\text{modified}}$ in relationship with relative slenderness $\bar{\lambda}_p$

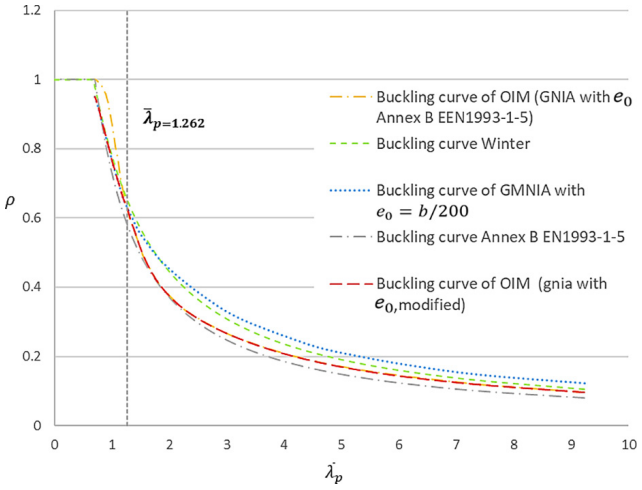

Fig. 23 Buckling curve of GMNIA, OIM with e_0, and OIM with $e_{0,\text{modified}}$ of unstiffened and square plate

application of Eq. (13) (Annex B of EN 1993-1-5 [10]), particularly assessing its conservative or unconservative outcomes across various slenderness ratios (b/t from 375 to 30). Additionally, the study investigated the influence of steel grade on plate behavior and its impact on e_0. This exploration facilitated modifications of e_0 within specific slenderness ranges, providing streamlined equations for applying GNIA with modified equivalent amplitudes in instances where unconservative buckling resistance values were obtained.

In scenarios involving unstiffened and square plates subjected to uniaxial compressive loads, the study meticulously examined the behavior concerning relative slenderness ($\bar{\lambda}_p$) for instances where $1.325 < \bar{\lambda}_p$, OIM's reduction factor and the values calculated using Eq. (13) closely aligned with Annex B of [10], albeit with a slightly less conservative stance. Conversely, when $1.325 > \bar{\lambda}_p \geq 0.7$, OIM's reduction factor surpassed those of GMNIA and Winter (Fig. 18). This discrepancy necessitated modifications, as outlined in Section 2.52 (Case S235).

The buckling resistance exhibited nuanced changes upon transitioning to the S355 material grade. For slenderness values falling within $1.3 < \bar{\lambda}_p$, OIM's reduction factor and the values derived from Eq. (13) closely mirrored Annex B of [10], albeit with a more lenient estimate. However, when $1.3 > \bar{\lambda}_p \geq 0.7$, OIM's reduction factor exceeded those of GMNIA and Winter (Fig. 13), demanding meticulous adjustments as detailed in Section 2.5.

In the context of steel grade S460, distinct alterations in behavior emerged. For relative slenderness between 1.262 and 0.7, OIM closely shadowed the predictions of Annex B of [10]. However, when $\bar{\lambda}_p$ surpassed 1.262, reaching values of ≥0.7, Eq. (13) required rigorous scrutiny and modification (Fig. 23, Section 2.5.3).

These findings emphasize the intricate balance required in applying OIM, particularly concerning material properties and slenderness ratios, underscoring the study's valuable contributions to structural engineering.

4 Conclusions

The primary focus of this study was to explore the viability of employing the (OIM) for plate buckling using Eq. (13) (Annex B of EN 1993-1-5 [10]). This equation, initially derived by Müller [20], was specifically tailored to calculate buckling resistance using the (GNIA), eliminating the need for complex analyses such as the Geometrically and Materially Nonlinear Imperfection Analysis (GMNIA). The research meticulously applied various methods outlined in EN 1993-1-5 [10], including GMNIA (Annex C of [10]), Winter's method (Section 4 of EN 1993-1-5 [10]), the Reduced Stress Method (Annex B of EN 1993-1-5 [10]), and OIM via Eq. (13) (Annex B of [10]). To assess the equation's accuracy, alterations in slenderness and material properties were systematically conducted in cases where Eq. (13) yielded non-conservative resistance values within specific slenderness ranges, and precise values for the imperfection amplitude (e_0) were determined. These calibrated values ensured that the calculated resistance aligned with GMNIA without surpassing the Winter curve. In summary, the study's findings provide crucial insights into the practical application of OIM, highlighting the significance of accurately determining imperfection parameters for robust structural analyses. Based on the findings presented in this study, several significant conclusions can be drawn:

- The GMNIA method, when utilizing equivalent geometric imperfections, exhibited consistent alignment with the winter curve across various steel grades (S235, S355, S460).
- Per Annex B of EN 1993-1-5 [10], the buckling curve consistently provided more conservative values than the winter curve, GMNIA, or OIM methods.
- The buckling curve derived from OIM yielded values that were more conservative than the winter or GMNIA methods but less conservative than Annex B of [10].
- The buckling curve of OIM became unconservative compared to winter or GMNIA beyond a specific value of relative slenderness.
- Altering the material resulted in a shift in the relative slenderness range, causing OIM to provide unconservative resistance values.
- The derived linear equation allows engineers to apply OIM without exceeding GMNIA's buckling curve, ensuring simplified application using GNIA.

Nomenclature

Latin upper case letters

A	cross-sectional area.
B	internal bimoment.
E	elastic modulus.
f_y	yield stress.
G	shear modulus.
I_y, I_z	moment of inertia with respect to y and z axes.
I_t	St. Venant torsional constant.
I_ω	warping moment of inertia.
L	length of members.
$M_{y,sec}$, $M_{z,sec}$	resistance to bending moments along both strong and weak cross-sectional axes.
M_{cr}	critical bending moment for lateral torsional buckling.
$M_{cr,NM}$	critical bending moment for coupled buckling.
$M^{II}_{\upsilon_{init}}$	2nd order bending moment regarding to υ^{II}.
$M^{II}_{\upsilon_{cr}}$	2nd order bending moment regarding to υ_{cr}.
$N_{cr,x}$	the essential elastic compressive force needed for torsional buckling exclusively around the longitudinal axis.
$N_{cr,y}$	the necessary elastic compressive force for inducing pure flexural buckling along the strong axis.
$N_{cr,z}$	the essential elastic compressive force needed to initiate pure flexural buckling along the weak axis.
$N_{cr,NM}$	critical force for coupled buckling.
W_y, W_z	section modulus regarding to y and z axes and the class of section.
U	the utilization of cross-sectional strength.

Latin lower case letters

a, b	dimension of plate.
r_0	polar radius of gyration.
t	thickness of the plate.
υ	full flexural deformation of members with imperfections.
υ^{II}	flexural 2nd order deformation of members with imperfections.
υ_{cr}	the shape's elastic buckling mode is related to bending.
υ''_{cr}	2nd derivative of υ_{cr}.
$\upsilon_{cr,\max}$	magnitude of υ_{cr}.
υ_{init}	initial flexural imperfection.
$\upsilon_{init,\max}$	magnitude of υ_{init}.
υ_{0d}	the equivalent magnitude of the original imperfection in terms of flexural buckling mode for the fundamental scenario of lateral-torsional buckling.
$\upsilon_{0d,NM}$	the magnitude that corresponds in terms of flexural behavior to the original imperfection, taking the form of a buckling mode, within the fundamental scenario of coupled buckling.
v	Poisson's ratio

Greek lower case letters

α	aspect ratio
α_b	amplification of the members' load to buckling mode.
α_{LT}	the parameter representing the degree of imperfection in the lateral torsional buckling curve.
α_{cr}	amplifier for the load that must be sustained by members in order to achieve the elastic critical buckling load.
α_{ult}	for the design loads to attain the characteristic resistance value at the member's most crucial place, the least load amplifier is necessary.
α_p	imperfection factor for plate buckling.
γ_{M_0}	cross-sectional resistance partial safety factor.
$\bar{\lambda}_{p0}$	global non-dimensional slenderness.
$\bar{\lambda}_p$	the plate slenderness for plate buckling.
μ	interaction parameter in the generalized imperfection factor.
$\sigma_{cr,p}$	elastic critical bulking stress in case of plate buckling.
$\sigma_{x,Ed}$, $\sigma_{z,Ed}$	design uniaxial and compressed stress in x and z direction.
ρ	reduction factor for plate buckling.

References

[1] CEN "EN 1993-1-1 Eurocode 3: Design of steel structures – Part 1-1: General rules and rules for buildings", European Committee for Standardization, Brussels, Belgium, 2005.

[2] Chladný, E., Štujberová, M. "Frames with unique global and local imperfection in the shape of the elastic buckling mode (Part 1)", Stahlbau, 82(8), pp. 609–617, 2013. https://doi.org/10.1002/stab.201310080

[3] Agüero, A., Pallarés, L., Pallarés, F. J. "Equivalent geometric imperfection definition in steel structures sensitive to flexural and/or torsional buckling due to compression", Engineering Structures, 96, pp. 160–177, 2015. https://doi.org/10.1016/j.engstruct.2015.03.065

[4] Papp, F. "Buckling assessment of steel members through overall imperfection method", Engineering Structures, 106, pp. 124–136, 2016. https://doi.org/10.1016/j.engstruct.2015.10.021

[5] Hajdú, G., Papp, F., Rubert, A. "Vollständige äquivalente Imperfektionsmethode für biege- und druckbeanspruchte Stahlträger" (Full equivalent imperfection method for steel beams subjected to bending and compression), Stahlbau, 86(6), pp. 483–496, 2017. (in German) https://doi.org/10.1002/stab.201710471

[6] Hajdú, G., Papp, F. "Safety Assessment of Different Stability Design Rules for Beam-columns", Structures, 14, pp. 376–388, 2018. https://doi.org/10.1016/j.istruc.2018.05.002

[7] Szalai, J., Papp, F. "New stability design methodology through overall linear buckling analysis", Ce/Papers, 3(3–4), pp. 859–864, 2019. https://doi.org/10.1002/cepa.1145

[8] Papp, F., Szalai, J., Majid, M. R. "Out-of-Plane Buckling Assessment of Frames through Overall Stability Design Method", Ce/Papers, 3(3–4), pp. 865–870, 2019. https://doi.org/10.1002/cepa.1146

[9] Nemer, S., Szalai, J. A., Papp, F. "The overall imperfection method or fire design situation", Engineering Structures, 283, 115884, 2023. https://doi.org/10.1016/j.engstruct.2023.115884

[10] CEN "EN 1993-1-5 Eurocode 3 - Design of Steel Structures - Part 1.5: Plated Structural Elements", European Committee for Standardization, Brussels, Belgium, 2006.

[11] Maquoi, R., Rondal, J. "Mise en equation des nouvelles courbes europeennes de flambement" (Equation of the new European buckling curves), Construction Métallique, 15(1), pp. 17–30, 1978. (in French)

[12] Riahi, F., Behravesh, A., Yousefzadeh Fard, M., Armaghani, A. "Buckling Stability Assessment of Plates with Various Boundary Conditions Under Normal and Shear Stresses", Engineering, Technology & Applied Science Research, 7(5), pp. 2056–2061, 2017. https://doi.org/10.48084/etasr.1516

[13] Beg, D., Kuhlmann, U., Davaine, L., Braun, B. "Design of plated structures: Eurocode 3: Design of steel structures, Part 1-5 – Design of plated structures", Ernst & Sohn, 2012. ISBN 9783433029800 https://doi.org/10.1002/9783433601143

[14] Dassault Systèmes "Abaqus 3DEXPERINECE R2019x", [computer program] Available at: https://blog.3ds.com/brands/simulia/r2019x-release-established-products/

[15] Zizza, A. "Buckling Behaviour of Unstiffened and Stiffened Steel Plates Under Multiaxial Stress States", Doctor of Engineering (Dr.-Ing.) Dissertation, Institut für Konstruktion und Entwurf der Universität Stuttgart, 2016. https://doi.org/10.18419/opus-8994

[16] Schönfeld, L., Naujoks, B., Ludwig, C. "Slenderness-dependent Equivalent Imperfections in Plate Buckling", Ce/Papers, 5(4), pp. 606–614, 2022. https://doi.org/10.1002/cepa.1797

[17] Braun, B. "Stability of Steel Plates under Combined Loading", Doctor of Engineering (Dr.-Ing.) Dissertation, Institut für Konstruktion und Entwurf der Universität Stuttgart, 2010. https://doi.org/10.18419/opus-349

[18] Rusch, A., Lindner, J. "Tragfähigkeit von beulgefährdeten Querschnittselementen unter Berücksichtigung von Imperfektionen" (Load-bearing capacity of cross-sectional elements at risk of buckling, taking imperfections into account), Stahlbau, 70(10), pp. 765–774, 2001. (in German) https://doi.org/10.1002/stab.200102520

[19] Python Software Foundation "Python 3.12" [computer program] Available at: https://www.python.org/downloads/release/python-312/

[20] Müller, C. "Zum Nachweis ebener Tragwerke aus Stahl gegen seitliches Ausweichen" (To Prove Flat Steel Structures against Lateral Deflection), PhD Thesis, RWTH Aachen University, 2003. (in German)

[21] Paudel, A., Gupta, S., Rowshan, N., Thapa, M., Mulani, S. B., Walters, R. W. "Stochastic Buckling of Composite Cylinder with Geometric Imperfection and Global Sensitivity Analysis", In: AIAA SCITECH 2023 Forum, National Harbor, MD, USA, 2023, AIAA 2023-1093. eISBN 978-1-62410-699-6 https://doi.org/10.2514/6.2023-1093

[22] Zhang, S., Xiao, H., Qiang, F., Hu, W. "Analytical Model and Numerical Simulation for the Effect of Uncertain Initial Geometrical Imperfection on the Buckling of Thin Plate", In: Proceedings of the 2017 5th International Conference on Frontiers of Manufacturing Science and Measuring Technology (FMSMT 2017), Taiyuan, China, 2017, pp. 738–745. ISBN 978-94-6252-331-9 https://doi.org/10.2991/fmsmt-17.2017.145

[23] Liu, L., Li, J.-M., Kardomateas, G. A. "Nonlinear vibration of a composite plate to harmonic excitation with initial geometric imperfection in thermal environments", Composite Structures, 209, pp. 401–423, 2019. https://doi.org/10.1016/j.compstruct.2018.10.101

[24] Zingoni, A. (ed.) "Advances in Engineering Materials, Structures and Systems: Innovations, Mechanics and Applications: Proceedings of the 7th International Conference on Structural Engineering, Mechanics and Computation (SEMC 2019), September 2-4, 2019, Cape Town, South Africa", [e-book] CRC Press, 2019. ISBN 9780429426506 https://doi.org/10.1201/9780429426506

[25] Radwan, M., Kövesdi, B. "Equivalent Geometric Imperfections for Local Buckling of Slender Box-section Columns", Periodica Polytechnica Civil Engineering, 65(4), pp. 1279–1287, 2021. https://doi.org/10.3311/PPci.18545

[26] Radwan, M., Kövesdi, B. "Equivalent geometrical imperfections for local and global interaction buckling of welded square box section columns", Structures, 48, pp. 1403–1419, 2023. https://doi.org/10.1016/j.istruc.2023.01.045

[27] Radwan, M., Kövesdi, B, "An Enhanced Design Approach for Global and Local Buckling Resistance of Welded Box Section Columns", Ce/Papers, 5(4), pp. 898–905, 2022. https://doi.org/10.1002/cepa.1833

[28] Radwan, M., Kövesdi, B. "Improved design method for interaction buckling resistance of welded box-section columns", Journal of Constructional Steel Research, 194, 107334, 2022. https://doi.org/10.1016/j.jcsr.2022.107334

[29] Wang, J., Di, J., Zhang, Q., Qin, F., Men, P. "Local buckling analysis of axially compressed welded box-section stub columns using Q420–Q960 steel", Journal of Constructional Steel Research, 210, 108100, 2023.
https://doi.org/10.1016/j.jcsr.2023.108100

[30] Somodi, B., Kövesdi, B., Hornyák, T. "Partial factor for local buckling of welded box sections", Structures, 30, pp. 440–454, 2021.
https://doi.org/10.1016/j.istruc.2021.01.004